Journal of Alloys and Compounds 509 (2011) 899–903

Contents lists available at ScienceDirect

Journal of Alloys and Compounds

journal homepage: www.elsevier.com/locate/jallcom

Electrochemical decomposition of SiO_2 pellets to form silicon in molten salts

Emre Ergül, İshak Karakaya*, Metehan Erdoğan

Middle East Technical University, Engineering Faculty, Department of Metallurgical and Materials Engineering, İnönü Bulvarı, 06531 Ankara, Turkey

ARTICLE INFO

Article history:
Received 8 July 2010
Received in revised form
22 September 2010
Accepted 22 September 2010
Available online 29 September 2010

Keywords:
Electrochemical reactions
Electrodeoxidation
Silicon
Silica
SiO_2
Molten salt

ABSTRACT

Direct electrochemical reduction of porous SiO_2 pellets in molten $CaCl_2$ salt and $CaCl_2$–NaCl salt mixture was investigated by applying 2.8 V potential. The study focused on the effects of temperature, particle size of SiO_2 powder starting material and the behavior of cathode contacting materials during electrochemical reduction process. The starting materials and the electrolysis products were characterized by X-ray diffraction analysis and scanning electron microscopy mainly. The studies showed that smaller particle sizes and higher temperatures had slightly positive effects in increasing the reduction rate within the ranges covered in this study. The results were interpreted from variations of current and accumulative electrical charge that passed through the cell as a function of duration of electrochemical reduction under different conditions. Microstructures and compositions of the reduced pellets were used to infer that electrochemical reduction of SiO_2 in molten salts may become a method to produce silicon that could be used in solar energy utilization. Furthermore, X-ray diffraction analysis results indicated that the silicon produced at the cathode reacts with contacting materials; nickel, and iron in stainless steel to form Ni–Si and Fe–Si compounds due to very reactive nature of silicon especially at high temperatures.

1. Introduction

Photovoltaic cells are considered as one of the promising solutions for energy and environmental issues. Clean and renewable energy can be produced by utilizing solar cells. As well as being an important part of the photovoltaic cells, solar grade silicon (SOG-Si) should be easily attainable for widespread usage of solar cells. The cost of conventional SOG-Si production is high due to processes which involve first conversion of raw Si into compounds such as; $SiHCl_3$, $SiCl_4$, SiH_2Cl_2, or SiH_4 and then transforming these silicon compounds back to high purity silicon [1]. Electrochemical methods have been considered as an alternative process, to reduce production cost of the solar grade silicon. Electrodeposition [2,3] and electrorefining [4] studies were carried out to obtain high purity silicon. However, feasible isolation of silicon with desired purity could not be achieved in these studies. Recently, a new study aiming at SOG-Si production was reported by Nohira et al. [5]. The study was based on electrodeoxidation of the oxide compound [6] in molten $CaCl_2$. After this report, several works related with the electrochemical reduction of SiO_2 to Si were reported [7–14]. A recent study [15] used a similar method with the addition of an yttria-stabilized zirconia oxygen ion conducting membrane in electrodeoxidation of SiO_2–TiO_2 mixture to form Si–Ti compounds by separating anode from molten electrolyte.

The reduction process of SiO_2 at the cathode is expressed as [8–10,12–14]:

$$SiO_2 + 4e^- \rightarrow Si + 2O^{2-} \quad (1)$$

A cyclic voltammetry study [16] showed the existence of above cathode reaction during decomposition of porous SiO_2. In addition, other cathode reactions, involving the formation of $CaSi_2$, Ca_2Si and Ca were reported at lower cathode potentials, corresponding to higher cell potentials.

Purity of the silicon is an important parameter for the production of SOG-Si. Therefore, particular attention should be given to the interactions between the cell components and the silicon. Silicon produced at the cathode is inevitably in contact with cathode contacting materials and the electrolyte. Molybdenum wire [5,8–10,13], nickel metal foil [7,11,12] and silicon plate [14] were used as the cathode contacting materials. Yet, the reported results do not comment adequately about the use of above metallic materials, except silicon, in the environments formed in these tests. Especially in the case of nickel and molybdenum that is in contact with elemental silicon, the formations of Ni_xSi_y and Mo_xSi_y intermetallics are inevitable [17,18]. In spite of this fact, only one study [11] mentioned that problem.

Furthermore, there are discrepancies about the rate of SiO_2 reduction in the literature. Only one of the reports [7] claims complete reduction of porous SiO_2 pellet to elemental Si. All other observations [5,8–14] give results of incomplete reductions. Although the reduction of bulk SiO_2 plates were claimed to be faster [10] than porous pellets, their reductions were still incomplete. In

---

* Corresponding author. Tel.: +90 3122102533; fax: +90 3122102518.
E-mail address: kkaya@metu.edu.tr (İ. Karakaya).

0925-8388/$ – see front matter © 2010 Elsevier B.V. All rights reserved.
doi:10.1016/j.jallcom.2010.09.126

addition, different colors reported for reduced products are; grey [7], red brick color [11], brown [16], and brownish as seen from reported photographs [5,8].

In the present study, electrochemical reduction of porous SiO_2 pellets was performed to examine the behavior of cathode materials and resolve the conflicts over the rate of reduction and the color of the products. Furthermore, the effects of reduction temperature and particle size of the SiO_2 powder starting material on the reduction of porous SiO_2 pellets in molten $CaCl_2$–NaCl salt mixture were investigated.

2. Experimental

The experimental set-up used in this study is a modified form of apparatus used before [19]. Detailed information about the experimental set-up and the procedure can be found elsewhere [20]. Brief information about the set-up and procedure is given below. Porous SiO_2 pellets were prepared by compressing about 1.20 grams of SiO_2 powder (Fluka 00653 purum p.a.; ≤230 mesh) into a cylindrical form under 1.5 t of load. Sintering at 1300 °C for 2 h resulted cylindrical pellets that had average diameters of 15 mm and heights of 5 mm. Silicon dioxide pellet, sandwiched between two contacting metal plates formed the cathode assembly. Plates were stainless steel, except in experiments that involved the study of the behavior of nickel cathode plate. One of the plates was welded to the end of the stainless steel wire (Ø: 3 mm, height: 60 cm) and placed under the pellet. The other plate was placed on top of the pellet. To hold this sandwiched structure together, a wire (Kanthal D, Ø: 0.15 mm) was wrapped around the plates. Two different procedures were employed to place the SiO_2 pellets in to the cathode assembly. Silica pellets were directly used in one, they were covered with a Kanthal wire (Kanthal D, Ø: 0.15 mm) mesh in the other procedure. The tests to examine the behavior of cathode contacting materials were done by using pellets without the wire mesh to have contact surface between the pellet and the contacting materials as much as possible. The wire mesh was used to decrease the contact surface between the pellet and contacting metal plates at the same time increase the electrolyte volume at SiO_2-cathode metal conductor–electrolyte interface. This procedure was expected to increase oxygen transport from the cathode and yield higher reduction rates.

The anode was prepared by connecting a 15 cm long and 13 mm diameter graphite (Alfa Aesar A10134) rod to a stainless steel wire (Ø: 3 mm, height: 45 cm). This assembly was covered with quartz to prevent short-circuiting of electrodes and undesired interactions with the gases formed inside the cell vessel. Both anode and cathode wires were extended out of the quartz cell vessel (50 mm outer diameter and 50 cm height) to enable easy connection to the power source. A Teflon lid was used to cover the quartz vessel at the top.

$CaCl_2$ (Riedel-de-Haën 12022) salt was dried before experiments under the vacuum by heating at a rate of 8 °C/h up to 400 °C to remove moisture. In some of the experiments $CaCl_2$ (70 mole%)–NaCl (Riedel-de-Haën 13423) (30 mole%) salt mixture was used as the electrolyte. About 100 g of salt was used in each experiment.

An alumina crucible with 4.5 cm outer diameter and 10 cm height filled with dried salt(s) was placed to the bottom of the cell vessel. The Teflon lid together with the anode and the cathode assemblies was then placed to the top of the vessel. The quartz vessel containing parts of the cell was placed into a Lindberg LHTF3226 vertical furnace. Argon inlet and gas outlet connections were established. A Eurotherm 818P unit was used to control the furnace temperature. It took about 2 h to attain a temperature around 800 °C. The whole heating processes and the electrolysis experiments were conducted under continuous flow of argon. When the cell reached the desired temperature, electrodes were immersed into the electrolyte. Sufficient period of time was given for the temperature and the composition to homogenize before the electrical connections to the cell were made. An Agilent N6700B low profile MPS main frame with N6773A direct current (DC) power module, power supply was used to apply 2.8 V potential between the cathode and the anode. The current passing through the cell was collected by a computer connected to the power supply via a visual basic code.

At the end of the experiments electrodes were lifted out of the electrolyte. After the system was cooled down, reduced pellets were taken out from the cathode. The product was washed in the ultrasonic water bed for 10 min to remove the remaining electrolyte from the pellet. Then, the reduced powder was put into about 200 ml hydrochloric acid solution that had 0.1 M concentration. The mixture was stirred for 20 min at room temperature to remove the calcium carbonate which was found in the reduced pellets. Characterization of the electrolysis products before and after the HCl treatment and the materials formed on the cathode contacting materials were done by XRD (Rigaku D/MAX2200/PC) and SEM (Nova NanoSEM 430, FEI) analysis.

3. Results and discussion

Electrochemical reduction of porous SiO_2 pellets were performed at 850 °C in $CaCl_2$ and 750 °C, 800 °C and 850 °C in $CaCl_2$–NaCl molten salt electrolytes. Two different particle sizes: smaller than 64 μm and smaller than 38 μm, were used. Fig. 1(a) shows the current versus time graphs of these reduction experiments. In order to show these results in a different way, and associate them with the amount of reduction, *W*, accumulative (total) charge, *Q*, passing through the cell, was calculated (shown in Fig. 1(b)) from;

$$Q = \int_0^t I dt = \frac{100WzF}{AX} \quad (2)$$

where *I* is the current in amperes, *t* is the time in seconds, *F* is the Faraday constant, *z* is the valence, *A* is the molecular weight of silicon dioxide and *X* is the percent current efficiency. The theoretical total charge required for the complete reduction of 1.2 g of SiO_2 was 7720 Coulombs (A s) as calculated from Eq. (2) by taking 100% current efficiency. Effects of temperature, electrolyte composition and particle size on the current and total charge that passed through the cell, shown in Fig. 1, were confirmed by repeated runs. As it is apparent from this figure, complete reduction of the pellets could not be achieved in any of the experiments. The highest total charge was observed during the experiment at 850 °C in $CaCl_2$ salt. Addition of NaCl decreased the value of *Q* at the same temperature of 850 °C. All experiments, except the one conducted at 850 °C in $CaCl_2$–NaCl salt mixture for 175 min, were conducted for 350 min.

The plots presented in Fig. 1(b) may be used to compare reduction rates of different runs when the same current efficiency is assumed. The $CaCl_2$ (70 mole%)–NaCl (30 mole%) salt mixture was used as the electrolyte to investigate the effect of temperature, for the first time. The experiments were conducted at 750 °C, 800 °C and 850 °C at 2.8 V. According to the graphs given in Fig. 1, temperature increase has a small positive effect in increasing the reduction rate in the temperature range studied. This increase was thought to be due to the increase in the diffusion of O^{2-} ions with increase in temperature. This result is consistent with the reported rate determining step of the electrodeoxidation process of SiO_2 [8], which is the diffusion of O^{2-} ions at the cathode. In the graphs of Fig. 1, it can also be seen that the reduction rate slightly increased with decreasing the particle size from sub-64 μm to sub-38 μm at 750 °C. This is in accord with the expectations, because smaller particle size yields condensed pellets that decrease the diffusion and the conduction paths.

The result of the test employing SiO_2 pellet with the Kanthal wire mesh is compared with SiO_2 pellet without the wire mesh in Fig. 2. Both data are from the experiments involving the same electrolyte composition, temperature, particle size and applied voltage. Since the reaction always starts where the contacting lead contacts the SiO_2 and the electrolyte, there are likely more contacts when Kanthal wire is wound round the sample. It is clear that employment of the Kanthal wire mesh increased the reduction rate by increasing oxygen transport from the cathode.

3.1. The rate of electrochemical reduction of porous SiO_2

Jin et al. [7] reported complete reduction of porous SiO_2 pellets to silicon at the end of 4 h of electrolysis. Contrary to this study, complete reduction of porous SiO_2 pellets with similar geometry and dimensions under the same applied DC potential, could not be achieved in 4 h in the present study. Only about half of the pellet was reduced at 850 °C, as deduced from Fig. 1. In the study of Pistorius and Fray, reduction of the porous SiO_2 pellets (Ø: 13.1 mm, height: 7.1 mm) to Si was achieved, but unreduced $CaSiO_3$ was reported. Their experiment probably continued for at least 16 h as can be deduced from their current versus time graphs. The presence of $CaSiO_3$ in their study may be the result of the reaction between the pellet and CaO.

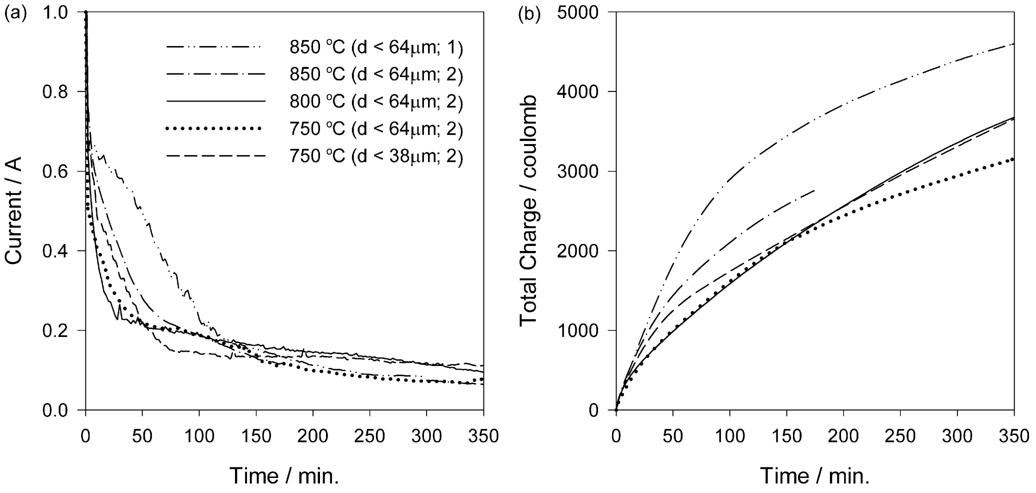

Fig. 1. (a) Current versus time and (b) total charge versus time graphs during the electrolysis of pellets under different conditions. All these tests were done with SiO_2 pellets, without the wire mesh, sandwiched between two stainless steel plates. Legends: d: particle size, 1: pure $CaCl_2$, 2: $CaCl_2$–NaCl electrolyte.

Table 1
ICP-MS results of Si powder.

Element	Concentration
Fe (%)	0.449 ± 0.005
Cr (%)	0.218 ± 0.005
Ni (μg/g)	64.10 ± 1.86

Electrolysis of porous SiO_2 pellets was performed at 750 °C by using 2.8 V applied potential for 4, 8 and 16 h to determine the required time for complete reduction in $CaCl_2$–NaCl salt mixture. In the experiments that continued for 4 and 8 h, the products contained unreduced SiO_2 together with Si and $CaCO_3$. Formation of calcium carbonate was thought to be due to the reaction between CaO and CO_2. CaO is normally present in $CaCl_2$ as it forms during the drying process. CO_2 was the product of graphite and O^{2-} ion carried to the anode in the electrolyte. $CaCO_3$ formation in CO_2 containing $CaCl_2$–CaO melts was reported before [11] and the reaction has negative standard Gibbs energy change [17].

The complete reduction of pellets (Ø: 15 mm, height: 5 mm), according to XRD results, were obtained in 16 h in the present study. The current efficiency calculated for complete reduction was above 90 percent. XRD analyses of the reduced products (Fig. 3(a)) showed the presence of neither the unreduced SiO_2 nor $CaSiO_3$. Only silicon and $CaCO_3$ were present. Absence of $CaSiO_3$ in all results (4, 8 and 16 h) of the present study may be attributed to low activity of CaO in anhydrous $CaCl_2$ used in this study. CaO activity in $CaCl_2$ was higher in the work of Pistorius and Fray [11] because they intentionally added CaO to the electrolyte.

3.2. The properties of produced silicon

After cleaning the product from calcium carbonate by HCl treatment, XRD analysis (Fig. 4) confirmed that the final product was silicon. SEM photograph and EDX analysis of the product are given in Fig. 5. The oxygen peak seen in EDX result was thought to be the result of the oxidation of silicon surface during washing and cleaning processes.

In order to determine the impurity level of the silicon due to contamination from the cathode contacting materials and other components of the cell, elemental analysis was conducted. For this purpose inductively coupled plasma-mass spectrometer (Perkin Elmer DRC II model ICP-MS) was used. The levels of important impurities; Fe, Ni and Cr are given in Table 1. Contamination by Fe was thought to be due to the stainless steel plates that were used to sandwich the Kanthal wire meshed pellet. Ni and Cr contaminations could be resulted from the stainless steel plates and Kanthal wire wrapping the pellet. These results indicate that purity of silicon is

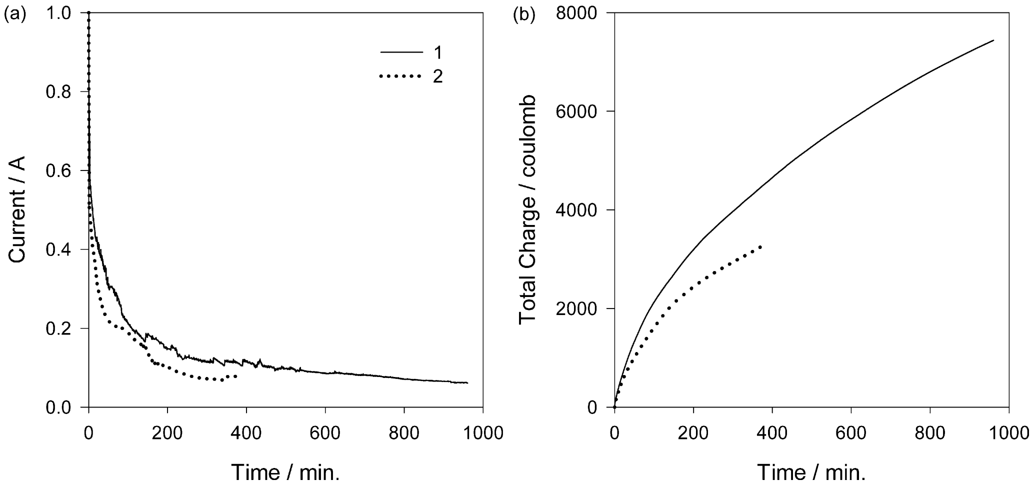

Fig. 2. (a) Current versus time and (b) total charge versus time graphs during the electrolysis of the pellets (1) with (2) without the Kanthal wire mesh (repeated from Fig. 1) sandwiched between two stainless steel plates. Both tests employed SiO_2 powder particle size less than 64 μm, $CaCl_2$–NaCl salt mixture at 750 °C and 2.8 V applied potential.

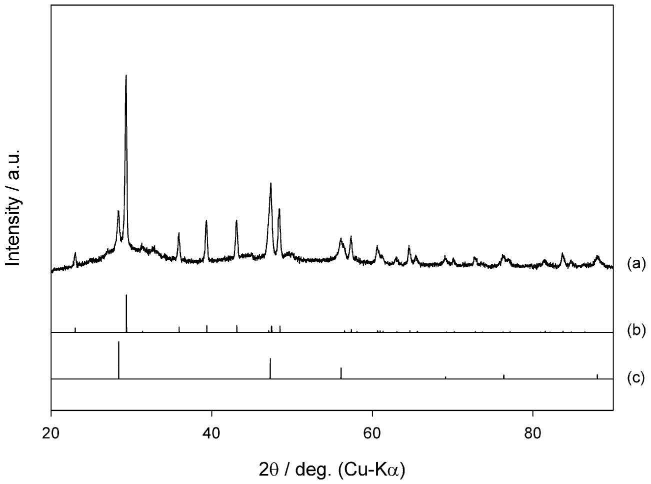

Fig. 3. (a) XRD pattern of the reduced pellet after 16 h of electrolysis, before the HCl treatment, (b) $CaCO_3$ (ICDD no: 5-0586) and (c) Si (ICDD no: 27-1402).

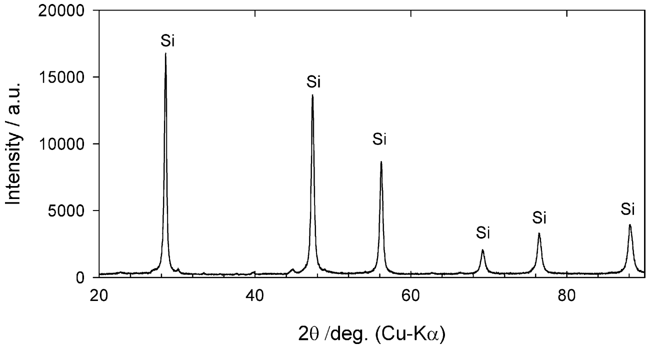

Fig. 4. XRD pattern of the reduced pellet after 16 h of electrolysis and the HCl treatment.

not in the desired range of SOG-Si. Improvements in materials used for cell components could lead to obtain higher purity silicon that may be used in solar energy utilization.

The color of the silicon powder obtained after HCl treatment of the electrochemically reduced samples was, unexpectedly, a tone of brown which is different from the gray color of bulk silicon. Brown color of silicon powder was reported in a recent study [16] when there was no calcium in the reduced samples. Brownish color was also observed from the photographs of the reduced products of some other studies [5,8]. Pistorius and Fray [11] reported a similar color, brick-red, in their study. However, the color of the silicon was reported as grey in the study of Jin et al. [7]. Pistorius and Fray [11] claimed that the brick-red color of the silicon may be due to an interference effect of silicon and calcium silicate mixture with very fine powder size. However, absence of calcium silicate in the products of the present study does not support this hypothesis. Silicon powders with brown color due to nanometer-scale crystallite size were reported in other studies [21,22]. In the light of these reports, crystallite size was calculated by using Maud program [23]. According to this calculation, crystallite size of the silicon produced in the present study was below 50 nm. Therefore, different tones of red and brownish color may be the result of the nanometer-scale crystallite size of the silicon powder.

3.3. The behavior of cathode contacting materials

In the study of Jin et al. [7], porous nickel foils were used as the cathode lead materials and porous SiO_2 pellet was sandwiched between these foils. They reported successful completion of electrochemical reduction of the pellet to silicon [7] in 4 h at 850 °C in pure $CaCl_2$ electrolyte. In the light of this study, porous SiO_2 pellet was placed between two nickel plates in the present study and 2.8 V electrical potential was applied between the electrodes for 4 h. At the end of the experiment, presence of a product other than the reduced pellet was observed on the nickel cathode plate under the pellet. Fig. 6(a) shows the XRD pattern of the material that was collected from the surface of nickel plate. XRD analysis confirmed the reduction of SiO_2, but also showed the presence of Ni–Si intermetallic compounds that could form by reactions between silicon and nickel. This result is supported by large negative Gibbs free energy of formation at 850 °C: −1624 and −134 kJ/mole [17] of $Ni_{31}Si_{12}$ and Ni_2Si, respectively. Ni–Si phase diagram [18] and Gibbs free energy of formation of Ni_2Si [17] were used to calculate the Gibbs free energy of formation of $Ni_{31}Si_{12}$. Formation of nickel silicide was also reported by Pistorius and Fray [11].

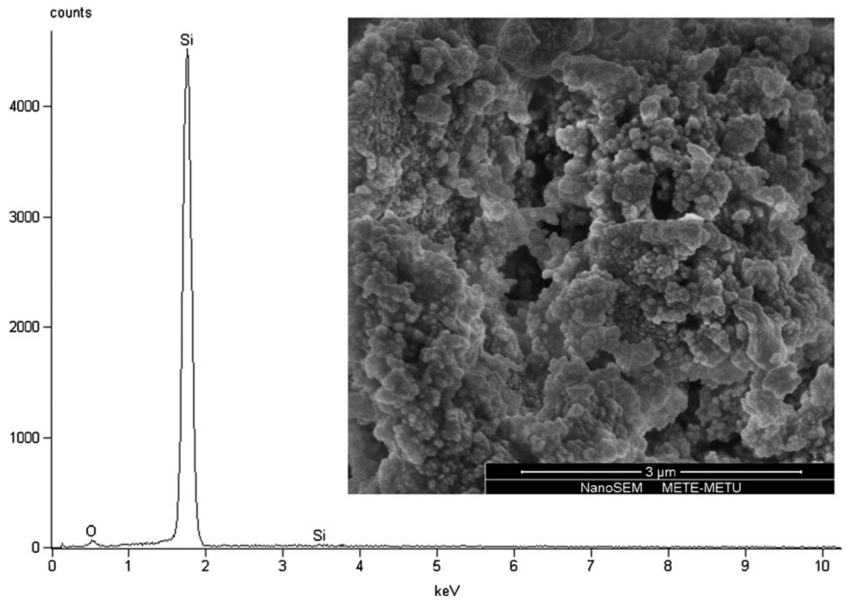

Fig. 5. EDX analysis and SEM photograph embedded into the EDX result frame of the sample produced after 16 h of electrolysis and HCl treatment.

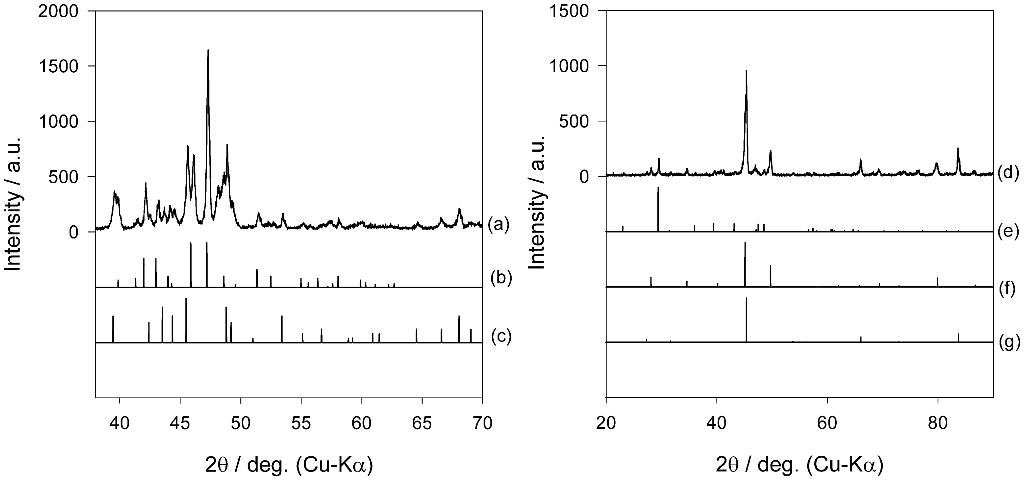

Fig. 6. XRD pattern of (a) the materials formed on the nickel plate, (b) $Ni_{31}Si_{12}$ (ICDD no: 17-0222), (c) Ni_2Si (ICDD no: 50-0779), (d) the materials formed on the stainless steel plate, (e) $CaCO_3$ (ICDD no: 5-0586), (f) FeSi (ICDD no: 38-1397) and (g) Fe_3Si (ICDD no: 45-1207).

Although the result could be anticipated because silicon forms stable compounds with iron, the behavior of the stainless steel plates were also tested in the environments formed during these experiments. A porous SiO_2 pellet was placed between two stainless steel plates and reduced for 4 h at 2.8 V. XRD analysis of the material collected from the surface of the stainless steel cathode contacting material revealed the presence of Fe–Si intermetallic compounds (Fig. 6(d)), as expected. Presence of some $CaCO_3$ was also observed in the XRD pattern.

From the observations of the amount of materials left under the reduced pellets and the intensities of the peaks given in Fig. 6, it was deduced that the loss of silicon was less when stainless steel plates were used as the cathode contacting materials.

4. Conclusions

Electrodeoxidation of porous SiO_2 pellets was investigated in molten $CaCl_2$ salt and $CaCl_2$–NaCl salt mixture. The effect of temperature on the electrochemical reduction of SiO_2 was studied by using $CaCl_2$–NaCl salt mixture as the electrolyte for the first time. A slight increase in the reduction rate, as deduced from total charge, could be attained with either increasing temperature from 750 °C to 850 °C or decreasing the SiO_2 particle size from sub-64 μm to sub-38 μm. Addition of NaCl to the electrolyte decreased the reduction rate.

Complete reduction of porous SiO_2 pellets was achieved after 16 h of electrolysis in the present study. The color of the silicon powder was a tone of brown. This color may be the result of nanometer-scale crystallite size of the silicon powder. Spectroscopic analysis revealed that the produced silicon was contaminated by the nickel and stainless steel plates which were used as the cathode contacting materials and does not meet the required specifications of SOG-Si. Impurity level of silicon may be reduced to the desired range for SOG-Si by advancement of the materials for the cell components.

Acknowledgment

Authors acknowledge the financial support provided by the Scientific and Technological Research Council of Türkiye (TÜBİTAK).

References

[1] W. Zulehner, Ullman's Encyclopedia of Industrial Chemistry, 5th ed., VHC, Weinheim, 1993.
[2] G.M. Rao, D. Elwell, R.S. Feigelson, J. Electrochem. Soc. 128 (1981) 1708–1711.
[3] R.C.D. Mattei, D. Elwell, R.S. Feigelson, J. Electrochem. Soc. 128 (1981) 1712–1714.
[4] I.G. Sharma, T.K. Mukherjee, Metall. Mater. Trans. B 17B (1986) 395.
[5] T. Nohira, K. Yasuda, Y. Ito, Nat. Mater. 2 (2003) 397–401.
[6] G.Z. Chen, D.J. Fray, T.W. Farthing, Nature 407 (2000) 361–364.
[7] X. Jin, P. Gao, D. Wang, X. Hu, G.Z. Chen, Angew. Chem. Ger. Ed. 43 (2004) 733–736.
[8] K. Yasuda, T. Nohira, K. Amezawa, Y.H. Ogata, Y. Ito, J. Electrochem. Soc. 152 (2005) D69–D74.
[9] K. Yasuda, T. Nohira, Y. Ito, J. Phys. Chem. Solids 66 (2005) 443–447.
[10] K. Yasuda, T. Nohira, K. Takahashi, R. Hagiwara, Y.H. Ogata, J. Electrochem. Soc. 152 (2005) D232–D237.
[11] P.C. Pistorius, D.J. Fray, J. S. Afr. I. Min. Metall. 106 (2006) 31–41.
[12] W. Xiao, X. Jin, Y. Deng, D. Wang, X. Hu, G.Z. Chen, Chemphyschem 7 (2006) 1750–1758.
[13] K. Yasuda, T. Nohira, R. Hagiwara, Y.H. Ogata, J. Electrochem. Soc. 154 (2007) E95–E101.
[14] K. Yasuda, T. Nohira, R. Hagiwara, Y.H. Ogata, Electrochim. Acta 53 (2007) 106–110.
[15] X. Zou, Lu, C. Li, Z. Zhou, Electrochim. Acta 55 (2010) 5173–5179.
[16] W. Xiao, X. Jin, Y. Deng, D. Wang, G.Z. Chen, J. Electroanal. Chem. 639 (2010) 130–140.
[17] I. Barin, O. Knacke, O. Kubaschewski, Thermochemical Properties of Inorganic Substances, Springer, Berlin, 1977.
[18] H. Baker (Ed.), ASM Handbook, ASM International, Ohio, 1993.
[19] M. Erdoğan, İ. Karakaya, Metall. Mater. Trans. B 41B (2010) 798–804.
[20] E. Ergül, İ. Karakaya, M. Erdoğan, in: B. Sopori, J. Yang, T. Surek, B. Dimmler (Eds.), Photovoltaic Materials and Manufacturing Issues II, Mater. Res. Soc. Symp. Proc. volume 1210, Warrendale, PA, 2010, 1210-Q08-17.
[21] H. Wiggers, R. Starke, P. Roth, Chem. Eng. Technol. 24 (2001) 261–264.
[22] E. Henneberg, J. Acker, I. Roever, G. Roewer, K. Bohmhammel, Thermochim. Acta 382 (2002) 297–301.
[23] L. Lutterotti, Nucl. Instrum. Methods B 268 (2010) 334–340.